Decision-Feedback Detection of Differential Unitary Space-Time Modulation in Fast Rayleigh-Fading Channels

Bijoy Bhukania and Phil Schniter*
The Ohio State University, Columbus, OH 43210

Abstract: With a fading channel, standard ML detection of Differential Unitary Space-Time Modulation (DUST) leads to an error floor in the BER-versus-SNR curve since it is derived under the assumption that the channel remains constant during every consecutive pair of matrix-symbols. In this paper, we present decision-feedback differential detection (DFDD) of DUST, which drastically reduces the error floor, especially in fast-fading channels. DFDD is derived from multiple-symbol ML detection and is shown to be equivalent to Wiener channel prediction followed by coherent ML detection. To derive the new detectors, we make the simplifying assumption that the channel changes once per matrix-symbol (i.e., block fading) rather than once per channel use (i.e., continuous fading). However, for the special case of diagonal space-time constellations, the block-fading assumption is not required. Exact and Chernoff bound expressions for pair-wise word-error probability (PWEP) are derived. An approximate expression for BER is derived from the PWEP which is in close agreement with the simulation results. The relationships between the performance and various system parameters, e.g., DFDD length, normalized Doppler frequency are then explored via numerical examples and related to the theoretical analysis.

1 Introduction

Differential Unitary Space-Time (DUST) modulation [1,2] is a multiple-antenna extension of differential phase-shift keying (DPSK). In DUST, the information is encoded in the phase difference between two consecutively transmitted $M \times M$ unitary matrix-symbols, where M is the number of transmit antennas. The standard single symbol ML detector, which detects one information matrix-symbol from each pair of consecutively received matrices, succumbs to an error floor in a fading channel [3–6]. For DPSK, multiple-symbol detection [5] and prediction-based decision-feedback detection [6] have been proposed to reduce, and asymptotically eliminate, the error floor in fading channels. Multiple-symbol detection has also been proposed for DUST in fast Rayleigh fading [7].

In this paper, we present decision-feedback differential detectors (DFDD) for DUST in fast Rayleigh-fading channels. In deriving the new detectors, we make the simplifying assumption that the channel changes once per matrix-symbol (i.e., M channel uses)[†] and that the receiver knows the fading correlation. Under these assumptions, a decision-feedback detector is derived from the multiple-symbol ML detector [7] and shown to be

*Direct all correspondence to: 205 Dreese Labs, 2015 Neil Avenue, Columbus, OH 43210. E-mail: schniter@ee.eng.ohio-state.edu.

[†]It can be shown that the block-fading assumption is not necessary when diagonal DUST constellations [1] are used [7].

equivalent to a Wiener-filter based channel predictor and detector. For performance analysis, exact and Chernoff bound expressions for pairwise word error probability (PWEP) are derived. An approximate expression for BER is then derived from the PWEP which is in close agreement with simulation results.

It may be worthwhile to mention a related work [8], wherein DFDD is proposed for the specific case of diagonal constellations, as opposed to the general case of unitary constellations [2, 9] which is our focus. Since diagonal DUST with M transmit antennas is equivalent to M decoupled single antenna DPSK systems, results for single antenna DPSK are trivially extended to diagonal DUST. Also, unlike [8], we derive the exact PWEP and hence obtain a better approximation of the BER.

The notations used in this paper are as follows: Matrices will be denoted by capital letters (e.g., X and $\mathbf{X}$) and column vectors by lower case bold (e.g., $\mathbf{x}$). $\mathbf{I}_P$ will denote identity matrix of size $P \times P$. The operator $\mathrm{vec}(\cdot)$, e.g., $\mathbf{x}_n = \mathrm{vec}(X_n)$, denotes stacking of the columns of matrix X_n in column vector $\mathbf{x}_n$. $(\cdot)^*$ denotes conjugate transposition, $\otimes$ denotes the Kronecker product, $\mathrm{tr}(\cdot)$ denotes the trace operator, $\det(\cdot)$ the determinant, and $\Re(\cdot)$ denotes the extraction of the real valued component. $\prod_{j=k_l}^{k_u} A_j = A_{k_l} A_{k_l+1} \cdots A_{k_u}$ if $k_u \geq k_l$, otherwise it denotes identity matrix of appropriate size, and $\hat{H}_n|_{k_l}^{k_u}$ denotes an estimate of H_n from the observations at time instant k_l through k_u.

2 System Model

We consider the system model

$$X_n = \sqrt{\frac{\rho}{M}} S_n H_n + W_n \tag{1}$$

where X_n is the $M \times P$ received matrix during the n^{th} matrix-symbol interval, and where M and P are the number of transmit and receive antennas, respectively. H_n is the $M \times P$ MIMO channel response matrix during the n^{th} matrix-symbol interval, containing i.i.d. unit variance proper complex Gaussian entries. S_n is the n^{th} $M \times M$ transmitted matrix-symbol, encoded as $S_n = V_{z_n} S_{n-1}$. $z_n \in \mathcal{L} = \{0, 1, \ldots, 2^{\eta M} - 1\}$ is the time-n integer index into matrix alphabet $\mathcal{A}$ of size $2^{\eta M}$, so that $V_{z_n} \in \mathcal{A}$. Thus η is the number of bits per channel use. S_n and V_{z_n} are unitary for all n, W_n is a matrix of i.i.d. unit variance proper complex Gaussian entries, and ρ is the average SNR per receive antenna.

Note that the system model (1) assumes that the channel H_n is fixed for M signaling intervals within the n^{th} matrix-symbol interval, i.e., the channel is block-fading. However, for the special case of diagonal codes, (1) can be shown to be a valid system model even in a continuously-fading channel such that the k^{th} row of H_n is the k^{th} row of $H_{k,n}$, where $H_{k,n}$ is the MIMO channel response matrix at the k^{th} time instant within the n^{th} matrix-symbol interval, i.e., at the $(nM + k)^{th}$ channel use [7]. Note that, if the MIMO fading process $H_{k,n}$ is independent between antennas, then H_n is also independent between antennas, and that (1) is an approximate model when non-diagonal constellations are used in continuous fading.

3 Decision-Feedback Differential Detection

3.1 DFDD from Multi-symbol ML Detection

Multiple symbol differential detection of DPSK and DUST has been proposed as an effective way to enhance performance in correlated Rayleigh fading [5, 7, 8]. The joint

ML detector of $\{z_k\}_{k=n-m+1}^{n}$ given the observation sequence $\{X_k\}_{k=n-m}^{n}$ is [7]

$$\{\hat{z}_k\}_{k=n-m+1}^{n} = \underset{z_n, z_{n-1}, \ldots \in \mathcal{L}}{\arg\max} \Re\left[\mathrm{tr}\left\{\sum_{k=0}^{m-1}\sum_{i=0}^{m-k-1} a_{i,i+k+1}^{(m)} X_{n-i}^{*}\left(\prod_{j=i}^{i+k} V_{z_{n-j}}\right) X_{n-i-k-1}\right\}\right] \quad (2)$$

where the combining coefficients $\{a_{i,j}^{(m)}\}$ are given by [7]

$$\begin{bmatrix} a_{0,0}^{(m)} & a_{0,1}^{(m)} & \ldots & a_{0,m}^{(m)} \\ a_{0,1}^{(m)*} & a_{1,1}^{(m)} & \ldots & a_{1,m}^{(m)} \\ \vdots & \vdots & \ddots & \vdots \\ a_{0,m}^{(m)*} & a_{1,m}^{(m)*} & \ldots & a_{m,m}^{(m)} \end{bmatrix} = -\left(\mathbf{I}_{m+1} + \frac{\rho}{M}\underbrace{\begin{bmatrix} \zeta_0 & \zeta_1 & \ldots & \zeta_m \\ \zeta_1^{*} & \zeta_0 & \ldots & \zeta_{m-1} \\ \vdots & \vdots & \ddots & \vdots \\ \zeta_m^{*} & \zeta_{m-1}^{*} & \ldots & \zeta_0 \end{bmatrix}}_{\Xi^{(m)}}\right)^{-1} \quad (3)$$

where ζ_k is defined such that $E[\mathbf{h}_n \mathbf{h}_{n-k}^{*}] = \zeta_k \mathbf{I}_{MP}$ for $\mathbf{h}_k = \mathrm{vec}(H_k)$. Note that $\zeta_0 = 1$ since H_k contains unit-variance entries.

The DFDD can be derived from the m-symbol ML detector (2) by feeding back the past decisions, i.e., replacing the hypotheses $\{z_k\}_{k=n-m+1}^{n-1}$ by the previously detected symbols $\{\hat{z}_k\}_{k=n-m+1}^{n-1}$ in the n^{th} symbol interval and maximizing the term on the right of (2) with respect to z_n alone. Of course, terms on the right of (2) that are not functions of z_n can be ignored. We denote the DFDD derived from the m-symbol ML detector as the m-DFDD, given by

$$\hat{z}_n = \underset{z_n \in \mathcal{L}}{\arg\max} \Re\left[\mathrm{tr}\left\{\sum_{k=0}^{m-1} a_{0,k+1}^{(m)} X_n^{*}\left(V_{z_n}\prod_{j=1}^{k} V_{\hat{z}_{n-j}}\right) X_{n-k-1}\right\}\right] \quad (4)$$

which is a generalization of the DFDD rules for DPSK [6] and diagonal constellations [8] to the general class of unitary constellations. It is not hard to show that when $\zeta_1 = 1$, 1-DFDD reduces to the "standard single symbol ML detector" (eq. (21) of [1]).

3.2 DFDD from MMSE channel prediction

Under the assumption of correct past decisions, i.e., $\hat{z}_k = z_k, k = n-m+1, \ldots, n-1$, we now derive a DFDD based on MMSE channel prediction. Although our derivations assume correct past decisions, the DFDD can be implemented in practice using symbol estimates.

In the symbol interval n we observe X_n for detection of V_{z_n}, and the observations $\{X_k\}_{k=n-m}^{n-1}$ are collected for estimation of H_n. For estimation of H_n we assume, for the moment, that $\{S_k\}_{k=n-m}^{n-1}$ is known (without error) at the receiver. We will see, however, that the resulting detector will depend on $\{V_{z_k}\}_{k=n-m+1}^{n}$ rather than $\{S_k\}_{k=n-m}^{n-1}$. Since $X_k = \sqrt{\frac{\rho}{M}} S_k H_k + W_k,\ k = n-m, \ldots, n-1$, denoting $\mathbf{h}_k = \mathrm{vec}(H_k)$, $\mathbf{x}_k = \mathrm{vec}(X_k)$, and $\mathbf{w}_k = \mathrm{vec}(W_k)$, we can write

$$\underbrace{\begin{bmatrix} \mathbf{x}_{n-1} \\ \vdots \\ \mathbf{x}_{n-m} \end{bmatrix}}_{\underline{\mathbf{x}}_{n-1}} = \sqrt{\frac{\rho}{M}}\underbrace{\begin{bmatrix} \mathbf{I}_P \otimes S_{n-1} & \mathbf{0} & \mathbf{0} \\ \mathbf{0} & \ddots & \mathbf{0} \\ \mathbf{0} & \mathbf{0} & \mathbf{I}_P \otimes S_{n-m} \end{bmatrix}}_{\mathcal{S}_{n-1}}\underbrace{\begin{bmatrix} \mathbf{h}_{n-1} \\ \vdots \\ \mathbf{h}_{n-m} \end{bmatrix}}_{\underline{\mathbf{h}}_{n-1}} + \underbrace{\begin{bmatrix} \mathbf{w}_{n-1} \\ \vdots \\ \mathbf{w}_{n-m} \end{bmatrix}}_{\underline{\mathbf{w}}_{n-1}} \quad (5)$$

Assume that the MMSE estimate of $\mathbf{h}_n$, $\hat{\mathbf{h}}_n = \mathrm{vec}(\hat{H}_n|_{n-m}^{n-1})$, is given by

$$\hat{\mathbf{h}}_n = \sum_{k=1}^{m} B_k^* \mathbf{x}_{n-k} = B^* \underline{\mathbf{x}}_{n-1} \tag{6}$$

where $B = [B_1^* \; B_2^* \; \ldots; B_m^*]^*$. It can be shown straightforwardly that the mean square error $J(B) = E[\|\hat{\mathbf{h}}_n - \mathbf{h}_n\|^2]$ is minimized by selecting

$$B = \sqrt{\frac{\rho}{M}} \mathcal{S}_{n-1} \left((T^{(m-1)^{-1}} \mathbf{g}) \otimes \mathbf{I}_{MP} \right) \tag{7}$$

where $\mathbf{g} = [\zeta_1 \; \zeta_2 \; \ldots \; \zeta_m]^*$, $T^{(m)} = \mathbf{I}_{m+1} + \frac{\rho}{M} \Xi^{(m)}$, and $\Xi^{(m)}$ is defined in (3). It can be shown that the minimum mean-square error $J_{\min}$ is given by $J_{\min} = MP \left(1 - \sigma_{\hat{H}}^2\right)$, where $\sigma_{\hat{H}}^2 = \frac{\rho}{M} \mathbf{g}^* T^{(m-1)^{-1}} \mathbf{g}$. The choice of the notation "$\sigma_{\hat{H}}^2$" will be made clear later. It can be shown that (for details, see [10])

$$\sqrt{\frac{\rho}{M}} (T^{(m-1)^{-1}} \mathbf{g}) \otimes \mathbf{I}_{MP} = \xi \begin{bmatrix} a_{0,1}^{(m)^*} \mathbf{I}_{MP} \\ \vdots \\ a_{0,m}^{(m)^*} \mathbf{I}_{MP} \end{bmatrix} \tag{8}$$

where $\xi = \sqrt{\frac{M}{\rho}} + \sqrt{\frac{\rho}{M}}(1 - \sigma_{\hat{H}}^2) > 0$. Therefore, the channel estimate $\hat{\mathbf{h}}_n$ is given by

$$\hat{\mathbf{h}}_n = \xi \sum_{k=0}^{m-1} a_{0,k+1}^{(m)} \left(\mathbf{I}_P \otimes S_{n-k-1}^* \right) \mathbf{x}_{n-k-1} \tag{9}$$

Defining the estimation error $\tilde{\mathbf{h}}_n = \mathbf{h}_n - \hat{\mathbf{h}}_n$, the system model (1) can be rewritten as

$$\mathbf{x}_n = \sqrt{\frac{\rho}{M}} \left(\mathbf{I}_P \otimes V_{z_n} \right) \left(\mathbf{I}_P \otimes S_{n-1} \right) \hat{\mathbf{h}}_n + \underbrace{\sqrt{\frac{\rho}{M}} \left(\mathbf{I}_P \otimes S_n \right) \tilde{\mathbf{h}}_n + \mathbf{w}_n}_{\tilde{\mathbf{w}}_n} \tag{10}$$

It is not hard to show that $E[\hat{\mathbf{h}}_n \hat{\mathbf{h}}_n^*] = \sigma_{\hat{H}}^2 \mathbf{I}_{MP}$ and $E[\hat{\mathbf{h}}_n \tilde{\mathbf{h}}_n^*] = \mathbf{0}$, which implies $E[\hat{\mathbf{h}}_n \tilde{\mathbf{w}}_n^*] = \mathbf{0}$. It can also be shown that $E[\tilde{\mathbf{w}}_n \tilde{\mathbf{w}}_n^*] = \sigma_{\tilde{W}}^2 \mathbf{I}_{MP}$, where $\sigma_{\tilde{W}}^2 = 1 + \frac{\rho}{M}(1 - \sigma_{\hat{H}}^2)$.

It is important to note that computation of the estimate $\hat{\mathbf{h}}_n$ requires the knowledge of the symbols $\{S_k\}_{k=n-m}^{n-1}$ which are unknown to the receiver, whereas $(\mathbf{I}_P \otimes S_{n-1}) \hat{\mathbf{h}}_n$ depends only on the previously detected (error-free) symbols $\{V_{z_k}\}_{k=n-m+1}^{n-1}$. Moreover, since the entries of $\tilde{\mathbf{h}}_n$ are zero-mean i.i.d. Gaussian variables, multiplication by the unitary matrix does not change its distribution. Therefore, from (10), the ML detector of V_{z_n} for known $(\mathbf{I}_P \otimes S_{n-1}) \hat{\mathbf{h}}_n$ is

$$\begin{aligned} \hat{z}_n &= \arg\max_{z_n \in \mathcal{L}} \Re \left[\mathbf{x}_n^* \left(\mathbf{I}_P \otimes V_{z_n} \right) \left(\mathbf{I}_P \otimes S_{n-1} \right) \hat{\mathbf{h}}_n \right] \\ &= \arg\max_{z_n \in \mathcal{L}} \Re \left[\mathrm{tr} \left\{ \xi \sum_{k=0}^{m-1} a_{0,k+1}^{(m)} X_n^* \left(V_{z_n} \prod_{j=1}^{k} V_{z_{n-j}} \right) X_{n-k-1} \right\} \right] \end{aligned} \tag{11}$$

which is identical to (4) under perfect past decisions since $\xi > 0$. Since perfect past decisions are not available in practice, (11) would be implemented using $\{\hat{z}_k\}_{k=n-m+1}^{n-1}$ in place of $\{z_k\}_{k=n-m+1}^{n-1}$, making it identical to (4).

Comment 3.1 : Though our derivations of DFDD for non-diagonal constellations assume block-fading channels, simulation results in Section 5 confirm that the m-DFDD for $m > 1$ derived in this paper significantly outperforms the standard single symbol detector under fast continuous-fading as well. Note that the coefficients $\{a_{i,j}^{(m)}\}$ used in the continuous-fading case would be recomputed with ζ_k defined such that $E[\mathbf{h}_{0,n}\mathbf{h}_{0,n-k}^*] = \zeta_k \mathbf{I}_{MP}$ for $\mathbf{h}_{0,n} = \mathrm{vec}(H_{0,n})$.

Comment 3.2 : The m-symbol ML detection rule (2) can be re-written as

$$\{\hat{z}_k\}_{k=n-m+1}^{n} = \underset{z_n, z_{n-1}, \ldots \in \mathcal{L}}{\arg\max} \Re\left[\mathrm{tr}\left\{\sum_{k=0}^{m-1} X_{n-k}^* V_{z_{n-k}} S_{n-k-1}(\hat{H}_{n-k}|_{n-m}^{n-k-1})\right\}\right] \quad (12)$$

$$\hat{H}_{n-k}|_{n-m}^{n-k-1} = \sum_{\ell=n-m}^{n-k-1} a_{k,n-\ell}^{(m)} S_\ell^* X_\ell \quad (13)$$

It is easy to show that the m-symbol ML detection rule for detecting $\{z_k\}_{k=n-m+1}^{n}$ from $\{X_k\}_{k=n-m+1}^{n}$ for known $S_{n-k-1}H_{n-k}$ can be written as (12) but with the replacement $\hat{H}_{n-k}|_{n-m}^{n-k-1} = H_{n-k}$. In fact, if $S_{n-k-1}\hat{H}_{n-k}|_{n-m}^{n-k-1}$ are any channel estimates such that the sum of the channel estimation error and the additive noise is white, then (12) is still the m-symbol ML detector. Thus we see that the multi-symbol ML detection rule has an estimator/detector structure, where the channel estimation is performed using (13).

4 Error Performance

In this section we first derive the exact PWEP and Chernoff upper bound expressions for genie-aided (i.e., perfect past decisions) DFDD, and later use them to approximate the BER.

4.1 Exact PWEP

Defining $\breve{\mathbf{h}}_n = \frac{1}{\sigma_{\hat{H}}}(\mathbf{I}_P \otimes S_{n-1})\hat{\mathbf{h}}_n$, $\breve{\mathbf{w}}_n = \tilde{\mathbf{w}}_n/\sigma_{\tilde{W}}$, and $\breve{\mathbf{x}}_n = \mathbf{x}_n/\sigma_{\tilde{W}}$ we can rewrite (10) as

$$\breve{\mathbf{x}}_n = \sqrt{\frac{\breve{\rho}}{M}}\,(\mathbf{I}_P \otimes V_{z_n})\,\breve{\mathbf{h}}_n + \breve{\mathbf{w}}_n \quad (14)$$

where $\breve{\rho} = \frac{\rho\sigma_{\hat{H}}^2}{\sigma_{\tilde{W}}^2}$ is the "equivalent SNR". Note that $\breve{\mathbf{h}}_n, \breve{\mathbf{w}}_n \sim \mathcal{CN}(\mathbf{0}, \mathbf{I}_{MP})$ and $E[\breve{\mathbf{h}}_n\breve{\mathbf{w}}_n^*] = \mathbf{0}$.

Given that the symbol V_1 was sent, the receiver will detect V_2, and thus make a decision error, if

$$\begin{aligned} \|\breve{\mathbf{x}}_n - \sqrt{\frac{\breve{\rho}}{M}}\,(\mathbf{I}_P \otimes V_2)\,\breve{\mathbf{h}}_n\|^2 &< \|\breve{\mathbf{x}}_n - \sqrt{\frac{\breve{\rho}}{M}}\,(\mathbf{I}_P \otimes V_1)\,\breve{\mathbf{h}}_n\|^2 \\ \Longleftrightarrow Q = [\mathbf{y}_1^*\ \mathbf{y}_2^*] \underbrace{\begin{bmatrix} \mathbf{I}_{MP} & \mathbf{0} \\ \mathbf{0} & -\mathbf{I}_{MP} \end{bmatrix}}_{K} \underbrace{\begin{bmatrix} \mathbf{y}_1 \\ \mathbf{y}_2 \end{bmatrix}}_{\mathbf{y}} &< 0 \end{aligned} \quad (15)$$

where $\mathbf{y}_1 = \sqrt{\frac{\breve{\rho}}{M}}\,(\mathbf{I}_P \otimes (V_1 - V_2))\,\breve{\mathbf{h}}_n + \breve{\mathbf{w}}_n$ and $\mathbf{y}_2 = \breve{\mathbf{w}}_n$, and the PWEP is given by

$$\Pr(V_1 \to V_2) = \Pr(Q \le 0) = \sum_{\substack{\text{poles } \omega = jp \\ p>0}} \mathrm{Res}\left[-\frac{\Phi_Q(\omega)}{\omega}\right] \quad (16)$$

where the summation is taken over the poles in the upper half plane (UHP) and $\Phi_Q(\omega) = E[e^{j\omega Q}]$. The characteristic function of Q, a Hermitian quadratic of Gaussian vector, is given by [11]

$$\Phi_Q(\omega) = \frac{1}{\det(\mathbf{I}_{2MP} - j\omega R_{\mathbf{y}} K)} \tag{17}$$

where $R_{\mathbf{y}} = E[\mathbf{y}\mathbf{y}^*]$, given as

$$R_{\mathbf{y}} = \begin{bmatrix} \frac{\breve{\rho}}{M}\left(\mathbf{I}_P \otimes (V_1 - V_2)(V_1 - V_2)^*\right) + \mathbf{I}_{MP} & \mathbf{I}_{MP} \\ \mathbf{I}_{MP} & \mathbf{I}_{MP} \end{bmatrix} \tag{18}$$

Using $\det \left[\begin{smallmatrix} A & C \\ B & D \end{smallmatrix}\right] = \det(A - BD^{-1}C)\det(D)$, it can be shown that [12]

$$\det(\mathbf{I}_{2MP} - j\omega R_{\mathbf{y}} K) = \prod_{k=1}^{M} \left(\frac{\breve{\rho}}{M}\sigma_k^2\right)^P (\omega - jp_k^+)^P (\omega - jp_k^-)^P \tag{19}$$

where σ_k is the k^{th} singular value of $V_1 - V_2$ and

$$p_k^{\pm} = \frac{1}{2}\left(1 \pm \sqrt{1 + \frac{4M}{\breve{\rho}\sigma_k^2}}\right)$$

Note that the characteristic function $\Phi_Q(\omega)$, and hence the PWEP, depend on the signal only through the singular values of $V_1 - V_2$. Since the singular values of $V_1 - V_2$ and $\mathbf{I}_M - V_2 V_1^*$ are the same, $\Pr(V_1 \to V_2) = \Pr(\mathbf{I}_M \to V_2 V_1^*)$.

Computation of the PWEP using (16) involves taking residues at poles with multiplicities greater than 1, which can be complicated. A simple method to evaluate the PWEP in such cases has been proposed in [12], where the poles are perturbed by small amount to eliminate multiplicity, and the PWEP is computed by taking residues at *all* the simple poles in UHP. This method produces an lower bound on the PWEP if all the concerned poles are moved away from origin, and upper bound when towards the origin. In this paper, the i^{th} occurrence of p_k^+ is replaced by $\tilde{\tilde{p}}_{(k-1)Pm_k+i}^+ = p_k^+ + (i-1)\epsilon_k$, yielding the set of simple poles $\{\tilde{\tilde{p}}_k\}_{k=1}^{MP}$, and hence, the PWEP from (16)

$$\Pr{}^{(L)/(U)}(V_1 \to V_2) \gtrless \sum_{k=1}^{MP} \frac{1}{\tilde{\tilde{p}}_k^+} \left(\prod_{\ell=1}^{M} \frac{M}{\breve{\rho}\sigma_\ell^2(\tilde{\tilde{p}}_k^+ - p_k^-)}\right)^P \prod_{\ell=1,\ell\neq k}^{MP} \frac{1}{(\tilde{\tilde{p}}_\ell^+ - \tilde{\tilde{p}}_k^+)} \tag{20}$$

where an upper bound is obtained by choosing $\epsilon_k = -0.0025\tilde{p}_k^+$, and a lower bound by choosing $\epsilon_k = 0.0025\tilde{p}_k^+$. Numerical results in Section 5 confirm that these bounds are very close to each other, and thus this method produces an accurate estimate of the PWEP.

4.2 Chernoff Bound on the PWEP

To obtain a better intuitive insight into the performance of DFDD, we now analyze the Chernoff upper bound on PWEP. Since (14) describes a known-channel system with equivalent SNR $\breve{\rho}$, the Chernoff bound on the PWEP is given by [1]

$$\Pr{}^{\text{Chernoff}}(V_1 \to V_2) \leq \frac{1}{2}\prod_{k=1}^{M}\left[1 + \frac{\breve{\rho}}{4M}\sigma_k^2\right]^{-P} \tag{21}$$

Observe that the diversity advantage of the system is MP, whereas the performance is governed by the equivalent SNR $\breve{\rho}$. Recall that $\breve{\rho}$ is a function of ρ, the SNR when the channel is known perfectly (henceforth termed "coherent SNR"), the length m of DFDD, and the fading correlations ζ_k.

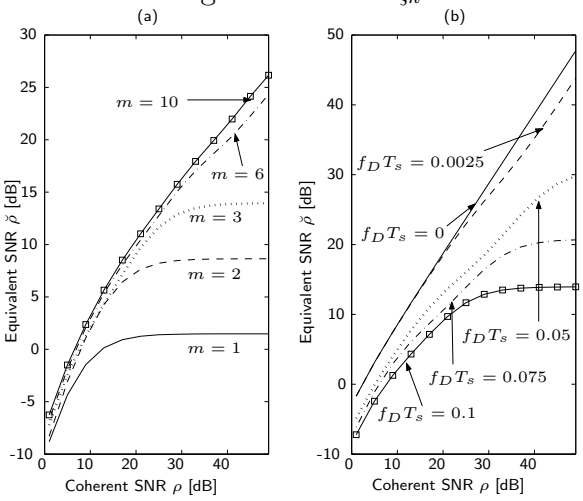

Figure 1: Equivalent SNR $\breve{\rho}$ vs coherent SNR ρ for (a) $f_D T_s = 0.1$, (b) $m = 3$.

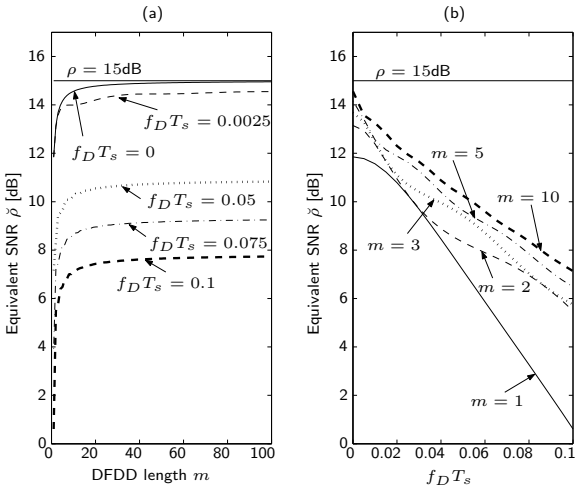

Figure 2: Equivalent SNR $\breve{\rho}$ vs (a) DFDD length m, (b) $f_D T_s$ for $\rho = 15$dB

For numerical examples in this paper, we consider a system with $M = 2$ transmit and $P = 2$ receive antennas. The MIMO channel exhibits Rayleigh fading [13] where the correlation between fading coefficients k matrix-symbols apart is given by $\zeta_k = J_0(2\pi f_D T_s M k)$ and where $f_D T_s$ is the normalized Doppler frequency. Observe that $f_D T_s M$ is the effective normalized Doppler frequency for $M \times M$ symbols. As we will see, the performance of the detectors degrades with increasing Doppler frequency, therefore, increasing M in a fading channel may degrade the performance.

Figure 1 demonstrates the variation of the equivalent SNR $\breve{\rho}$ w.r.t. the coherent SNR ρ for different $f_D T_s$ and DFDD feedback lengths m. Observe that when either $f_D T_s$ is large or m is small, $\breve{\rho}$ reaches a ceiling, implying that an error floor will appear in the BER vs. SNR ρ curve. Fig. 1(a) indicates that increasing m has less pronounced effect on the performance when ρ in small, whereas the performance improvement can be significant when ρ is high. Equation (21) and Fig. 1(b) imply that the slope of the BER vs coherent SNR ρ curve would decrease with increasing $f_D T_s$, which is in accordance with the result for DPSK reported in [6].

Figure 2 examines variations in $\breve{\rho}$ versus m and $f_D T_s$ for $\rho = 15$dB. Fig. 2 indicates that increasing m beyond, say, $m = 10$ has an insignificant effect on performance. Note also that when $f_D T_s = 0$, coherent detection performance is achieved asymptotically by DFDD. Performance loss due to increased channel variation is depicted in Fig. 2(b).

4.3 Approximate Bit Error Rate

In practice, bit error probability (BER) is a more useful metric than PWEP. Since $\Pr(V_1 \to V_2) = \Pr(\mathbf{I}_M \to V_2 V_1^*)$, and $V_1, V_2 \in \mathcal{A} \implies V_2 V_1^* \in \mathcal{A}$, and since ηM bits are encoded in each transmitted matrix-symbol, under the assumption of Gray mapping and equal prior probabilities the BER can be written as

$$P_{\text{genie}}^{\text{Chernoff}/(L)/(U)} \approx \frac{1}{\eta M} \sum_{j=1}^{2^{\eta M}-1} d(\mathbf{I}_M, V_j) \Pr^{\text{Chernoff}/(L)/(U)}(\mathbf{I}_M \to V_j) \tag{22}$$

where $d(V_j, V_k)$ is the Hamming distance between the binary representations of V_j and V_k, and $\Pr^{\text{Chernoff}/(L)/(U)}$ from (20) & (21) are used.

For realizable m-DFDD, the influence of incorrect past-decisions has to be taken into account for $m > 1$. In [14] it has been shown that the BER of realizable DFDD is approximately twice that of genie-aided DFDD for DPSK, since every error is likely to cause another error due to error propagation. Through numerical evaluation we find that this approximation extends to DUST as well, which is in accordance with [8].

5 Simulations & Numerical Results

We evaluate the performance of the detectors with two channel types: "block fading" and "continuous fading". In continuous fading the correlation between coefficients k symbols apart is given by $J_0(2\pi f_D T_s k)$ [13], while, in block-fading, the correlation between channel coefficients m matrix-symbols apart is given by $J_0(2\pi f_D T_s M m)$.

Since the use of diagonal constellations in continuous fading yields the same model as general constellations in block fading [7], detector performance is identical in these two cases. Therefore, we focus on detector performance using diagonal and non-diagonal constellations in continuous fading. We consider a system with two receive antennas and use the constellations specified in [1] with two transmit antennas and $\eta = 1$.

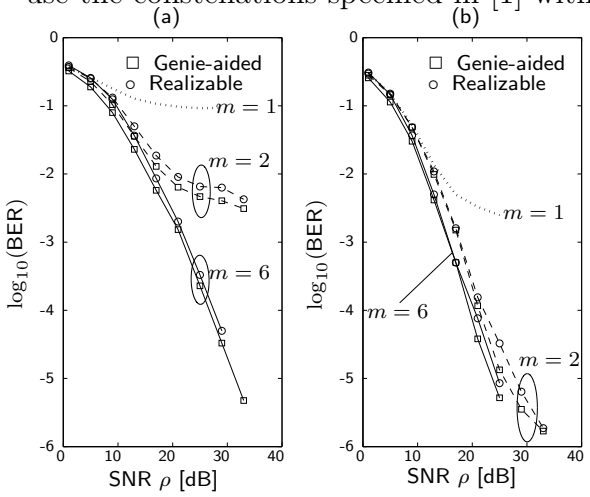

Figure 3: m-DFDD detection of diagonal constellation in continuous fading with (a) $f_D T_s = 0.1$, (b) $f_D T_s = 0.05$

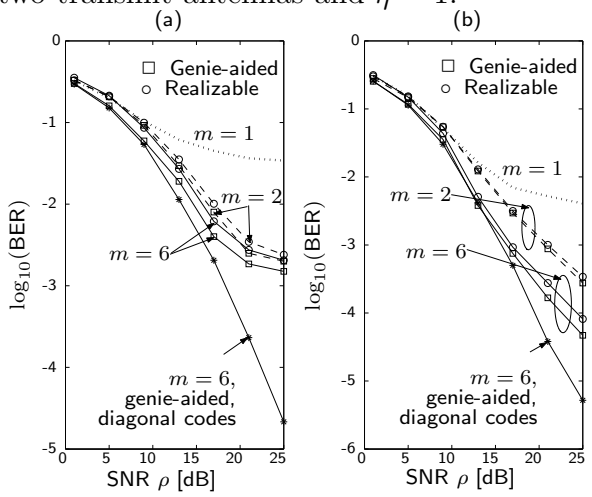

Figure 4: m-DFDD detection of non-diagonal constellation in continuous fading with (a) $f_D T_s = 0.075$, (b) $f_D T_s = 0.05$

The simulated BER of genie-aided as well as realizable 1-, 2-, and 6-DFDD in continuous fading with $f_D T_s = 0.1$ and 0.05 is shown in Fig. 3, where the advantage of m-DFDD, $m > 1$ over standard single symbol detection is clearly illustrated. When $f_D T_s = 0.1$, 1-DFDD, which is equivalent to standard single symbol detection, succumbs to very high error floor, whereas the performance is dramatically improved when 6-DFDD is employed, as predicted by Fig. 1(a). Meanwhile, 2-DFDD performs much better than 1-DFDD while still succumbing to an error floor. Similar, though less pronounced, trends can be seen in Fig. 3(b), where $f_D T_s = 0.05$. Figure 3 also demonstrates the effect of error propagation via comparison of genie-aided and realizable DFDD.

Next, the performance of the detectors has been evaluated in continuous fading with a non-diagonal constellation to illustrate the performance loss due to approximation in system model (1). The non-diagonal constellation is generated by right multiplying the diagonal constellation by a fixed non-diagonal unitary matrix. Because such an operation

does not change the product distance of the constellation [1], the comparison is fair.

Figure 4 illustrates the performance of 1-,2-, and 6-DFDD using the non-diagonal constellation in continuous fading with $f_D T_s = 0.075$ and $f_D T_s = 0.05$. Although a performance loss is incurred due to neglecting the channel variation within the matrix-symbol interval, in both cases 2- and 6-DFDD perform much better than single symbol detection. Unlike diagonal constellation case, Fig. 4 shows that 6-DFDD provides significant performance gain over 2-DFDD when $f_D T_s = 0.05$, whereas the gain is insignificant for higher $f_D T_s$.

Now we compare theoretical with simulated BER to verify the validity of the error analysis in Section 4. Since BER and PWEP expressions have been derived for genie-aided DFDD, and since the approximate BER of realizable DFDD can be obtained by multiplying the genie-aided BER by 2 [8,14], we present simulation and theoretical results for only the genie-aided case.

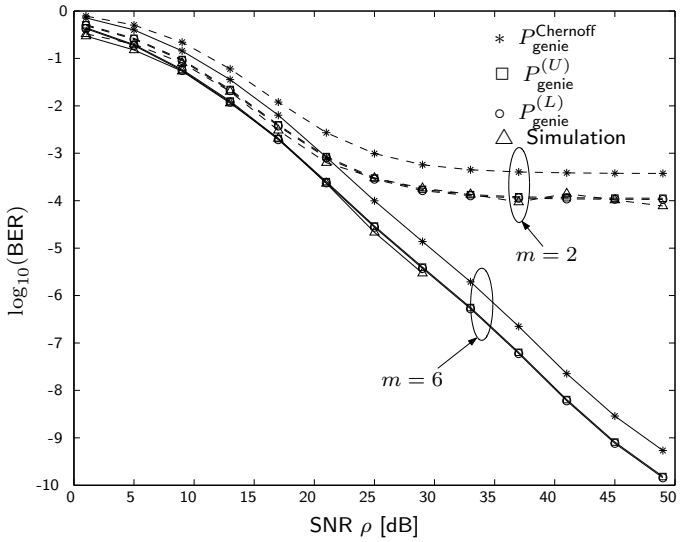

Figure 5: Theoretical and simulated BER of genie-aided m-DFDD: Diagonal constellation in continuous fading with $f_D T_s = 0.075$

Figure 5 compares the theoretical and simulated BER of 2- and 6-DFDD using a diagonal constellation in continuous fading with $f_D T_s = 0.075$. Three approximations to the BER, $P_{\text{genie}}^{\text{Chernoff}}$, $P_{\text{genie}}^{(L)}$, and $P_{\text{genie}}^{(U)}$ from (22) are presented. Observe that $P_{\text{genie}}^{(L)}$ and $P_{\text{genie}}^{(U)}$ are somewhat loose at high BER since (22) employs the union bound, whereas at lower BER these approximations closely matches the simulated BER. Since $P_{\text{genie}}^{(L)}$ and $P_{\text{genie}}^{(U)}$ are very close to each other, in practice either one of them can be used for error analysis.

6 Conclusions

In this paper, we have demonstrated, via simulation as well as theoretical error performance analysis, the efficacy of decision-feedback differential detection for DUST modulation in fast-fading channels. Although the DFDDs assume the channel to be block-fading when non-diagonal constellations are used, they have been shown to improve the performance in continuous fading as well. The m-DFDD performance has been shown to degrade with increasing Doppler frequency, and improve with increasing m.

References

[1] B. M. Hochwald and W. Sweldens, "Differential unitary space-time modulation," *IEEE Trans. on Communications*, vol. 48, pp. 2041–2052, Dec. 2000.

[2] B. L. Hughes, "Differential space-time modulation," *IEEE Trans. on Information Theory*, vol. 46, pp. 2567–2578, Nov. 2000.

[3] P. Bello and B. Nelin, "The influence of fading spectrum on the binary error probabilities of incoherent and differentially coherent matched filter receivers," vol. CS-10, pp. 160–168, June 1962.

[4] C. Peel and A. Swindlehurst, "Performance of unitary space-time modulation in continuously changing channel," in *Proc. IEEE Internat. Conf. on Acoustics, Speech, and Signal Processing*, 2001.

[5] P. Ho and D. Fung, "Error performance of multiple symbol differential detection of PSK signals transmitted over correlated Rayleigh fading channels," *Proc. IEEE Intern. Conf. on Communication*, vol. 2, pp. 568 –574, 1991.

[6] R. Schober, W. Gerstacker, and J. Huber, "Decision feedback differential detection of MDPSK for flat Rayleigh fading channels," *IEEE Trans. on Communications*, vol. 47, pp. 1025–1035, July 1999.

[7] B. Bhukania and P. Schniter, "Multiple-symbol detection of differential unitary space-time modulation in fast Rayleigh-fading channels." Submitted to *IEEE Trans. on Communications*, April 2002.

[8] R. Schober and H.-J. Lampe, "Noncoherent receivers for differential space-time modulation," *Proc. IEEE Global Telecommunications Conf.*, vol. 2, pp. 1127–1131, 2001.

[9] G. G. abd P. Stoica, "Differential modulation using space-time block codes," *IEEE Signal Processing Letters*, vol. 9, pp. 57–60, FEB. 2002.

[10] B. Bhukania and P. Schniter, "Decision feedback detection of differential unitary space-time modulation in fast Rayleigh-fading channels." Submitted to *IEEE Trans. on Communications*, July 2002.

[11] G. Turin, "The characteristic function of Hermitian quadratic forms in complex normal variables," *Biometrika*, pp. 199–201, 1960.

[12] S. Siwamogsatham, M. Fitz, and J. Grimm, "A new view of performance analysis of transmit diversity schemes in correlated Rayleigh fading," *IEEE Trans. on Information Theory*, vol. 48, pp. 950–956, April 2002.

[13] W. Jakes, *Microwave Mobile Communications*. Piscataway, NJ: IEEE press, 1993.

[14] F. Edbauer, "Bit error rate of binary and quaternary DPSK signals with multiple differential feedback detection," *IEEE Trans. on Communications*, vol. 40, pp. 457–460, March 1992.